AUTOMATIC IMAGE-TO-WORLD REGISTRATION BASED ON X-RAY PROJECTIONS IN CONE-BEAM CT

N. M. Hamming[1], M. J. Daly[2], J. C. Irish[2], J. H. Siewerdsen[3],
[1]Centre for Global eHealth Innovation, UHN, Toronto, ON, Canada
[2]Ontario Cancer Institute, PMH, Toronto, ON, Canada
[3]Department of Biomedical Engineering, JHU, Baltimore, MD, USA

I. INTRODUCTION

Image-guided surgery (IGS) is becoming common to the modern surgical arsenal for a variety of procedures in orthopaedic-, neuro-, and ENT surgeries.[1-2] Conventionally, IGS utilizes preoperative CT or MRI images to assist the surgeon in planning and execution of a surgical procedure with increased precision and accuracy by helping to resolve geometric uncertainties. More recently, intraoperative imaging and real-time surgical navigation technologies are being realized that allow guidance with respect to images that accurately reflect morphological change and surgical tool placement at the time of surgery.

Surgical navigation requires registration of image and tracking coordinate systems, known as image-to-world registration. Conventionally, markers are localized manually in the image (mouse-click) and tracking (trackable pointer) coordinates. The timescale associated with manual co-localization is long (minutes) and can present a bottleneck to surgical workflow. Intraoperative imaging not only provides images that accurately reflect morphological changes, it also presents a means to conduct image-to-world registration automatically based on markers that are visible to both the imaging and tracking systems.

II. MATERIALS

A. Intraoperative Cone-Beam CT (CBCT)

A mobile C-arm for intraoperative CBCT has been developed in collaboration with Siemens Healthcare as previously described[3] and illustrated in Fig. 1(a). The main modifications include: replacement of the x-ray image intensifier with a large-area, flat-panel detector (FPD) (Varian PaxScan 4030CB) allowing a field-of-view (FOV) of 20x20x15cm^3 and soft-tissue imaging capability; motorization of the C-arm orbit and development of a geometric calibration method;[4] and integration with a computer-control system for image readout and 3D reconstruction.

B. Tracking System and Multi-Modality Markers

The infrared (IR) tracking system (NDI Polaris Vicra) illustrated in Fig. 1(a) was used to measure the position of reflective spherical markers. The markers were affixed to trackable tools or objects, Fig 1(b). A reference tool was used with the tracking system to ensure that perturbation of the camera or object would not result in loss of registration.

Multi-modality (MM) markers were designed to allow localization by both the IR tracking system and the x-ray imaging system. As illustrated in Fig. 1(c), each MM marker consists of a 2.0 mm diameter tungsten sphere (BB) at the center of a reflective spherical marker mounted on an x-ray translucent support. The centers of the BB and reflective markers are coincident within 0.15±0.04 mm. In the automatic image-to-world registration, the BB markers are localized in CBCT projection data ("image point-set") which is rigidly registered to reflective markers localized by the tracking system ("tracker point-set").

C. Anthropomorphic Head Phantom

As shown in Fig. 1(b), an anthropomorphic head phantom containing a natural human skeleton and soft-tissue-simulating material was used to provide a realistic context in which to develop and evaluate the automatic registration algorithm. The head was rigidly mounted in an acrylic frame, with the reference tool

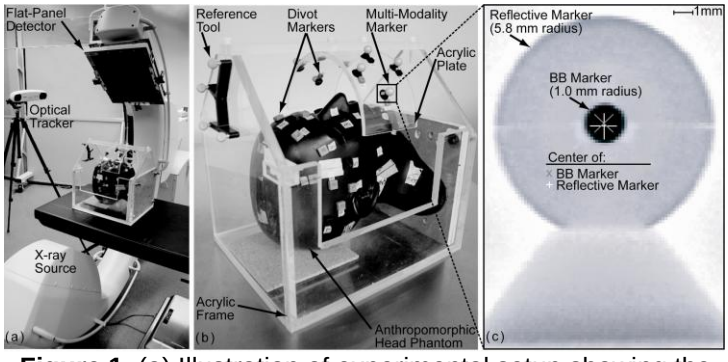

Figure 1. (a) Illustration of experimental setup showing the C-arm, optical tracking system, and head phantom. (b) Close up of the head phantom setup. Divot markers used to manually localize landmarks and target points; MM markers used in automatic registration. (c) Radiograph of MM markers mounted on an x-ray translucent post. Markers consist of a reflective spherical marker with tungsten sphere (BB) placed at center. The gray 'X' and white '+' indicate the BB marker and reflective marker centers, respectively.

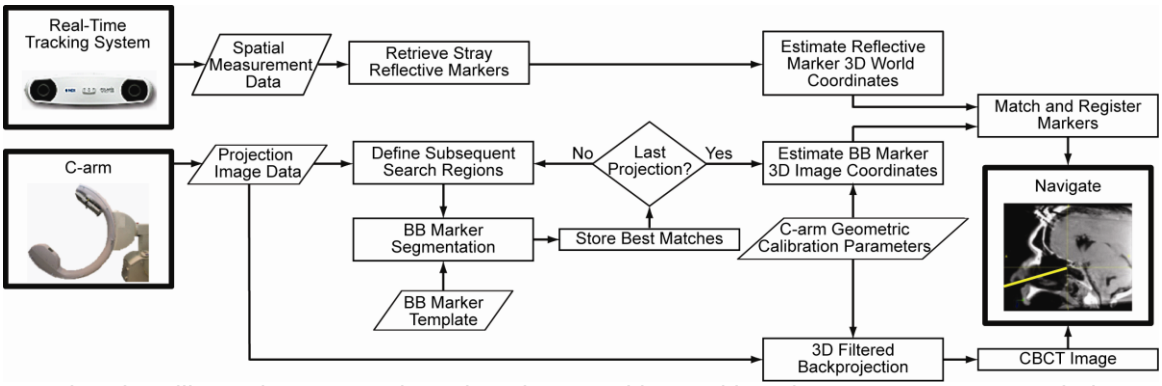

Figure 2. Flowchart illustrating automatic registration. Tracking and imaging processes operate independently up to marker matching and registration. The tracking system localizes the reflective markers. The imaging system searches each projection for BB markers and transforms to the 3D location using the C-arm geometric calibration. Image and tracker point-sets are registered, and then surgical navigation can proceed.

attached. The frame incorporated a curved acrylic plate placed over the head phantom as illustrated in Fig. 1(b). Two types of markers were affixed to the head and/or the curved plate – the MM markers (used for automatic localization) and divot markers (used for manual localization). In addition, 4 divot markers on skin surface represented targets for evaluation of target registration error (TRE).

III. AUTOMATIC IMAGE-TO-WORLD REGISTRATION ALGORITHM

Automatic registration consists of processes illustrated in Fig. 2 to localize markers in both the image and world reference frames. Markers are first localized within 2D projections, then transformed to 3D image coordinates, via the geometric calibration of the C-arm, and finally matched and registered to the tracker point-set to allow surgical navigation.

A. 3D Localization of Reflective Markers

The tracking system is capable of localizing up to 50 reflective spherical markers within its FOV. The locations of the MM markers are retrieved through an application program interface command to the camera.

B. 3D Localization of BB Markers

Localization of the BB markers in 3D image coordinates is a two-step process: i.) segmentation of BBs in the 2D projection image data, followed by ii.) estimation of BB locations in 3D image coordinates.

Figure 3(a) shows a CBCT projection of the MM markers affixed to the surface of the head phantom, from which the coordinates of the BBs may be determined by intensity thresholding and template matching. In each projection (nominally 200), the centroids of all template-matched objects are calculated, and the FPD pixel location is stored.

Definition of constrained search regions was found to reduce the complexity of BB segmentation and improve the robustness of automatic 2D localization. Following initial localization of a BB marker in 2D, and using the corresponding estimate of its 3D location, the position of the marker in the subsequent projection can be predicted by forward projection. A constrained search window can therefore be defined in which a BB marker is expected to appear in subsequent projections. In addition, search regions at the left and right edge of the projection were defined to better detect BBs entering the 2D FOV. Any area of the edge search region that overlaps a search window is omitted during segmentation.

The 3D image coordinate location of each BB centroid is estimated by transforming the 2D FPD pixel locations in each projection using the C-arm geometric calibration and a linear least squares (LLS) method. First, the C-arm geometric calibration is used to determine the position of the segmented BB centroids in the FPD coordinate system.[4] The FPD position of the BB is then transformed to the image coordinate system to determine the position of the BB on the FPD surface, as illustrated in Fig. 3(c). The 3D image

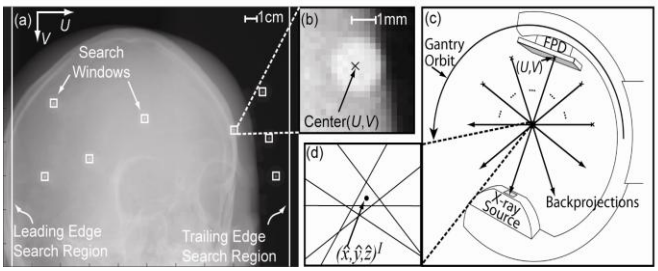

Figure 3. Determination of marker locations from 2D projections. (a) Segmentation of BB markers in 2D projection by intensity thresholding and pattern matching. (b) Example search window for BB segmentation. (c) Estimation of BB marker 3D location. (d) The 3D estimate of marker location is the point of minimum distance from all backprojections over the gantry orbit.

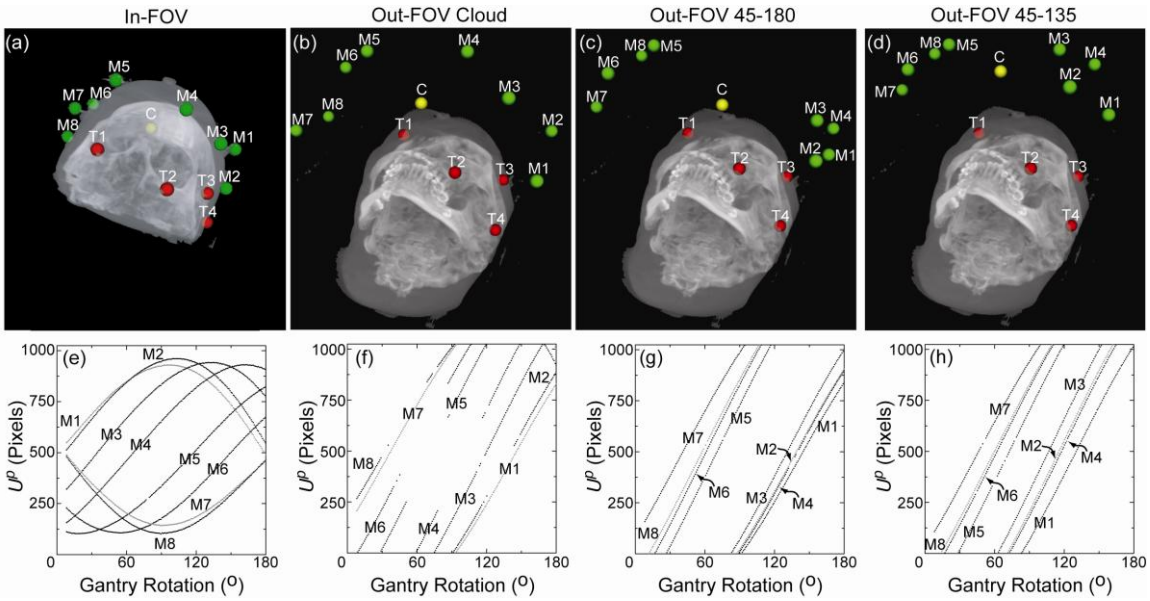

Figure 4. Illustration of marker configurations, targets, and location of segmented BB centroids. Images (a)-(d) show maximum intensity projections renderings of CBCT images superimposed with the locations of 8 MM markers (M1-M8, green), configuration centroid of the markers (C, yellow), and the 4 target points (T1-T4, red). "In-FOV" configurations involve MM markers affixed to the surface of the phantom, while "Out-FOV" configurations involve markers affixed to a curved acrylic plate [Fig. 1(b)] such that markers are present only in a subset of projections. The plots of (e)-(h) show the U^p coordinate of each of the markers versus the C-arm rotation angle.

coordinate of the BB lies somewhere along the line-segment from the surface position to the x-ray source.

In an ideal system, backprojected lines from a given marker's location in each projection over the gantry orbit would intersect at a common point. Due to non-idealities in the C-arm gantry rotation and inaccuracy in the 2D segmentation process, however, these backprojected lines do not perfectly intersect, as illustrated in Fig. 3(d). Therefore, a LLS method was employed to determine the point of minimum distance from all backprojected lines from a set of projections in which the BB was segmented.

C. Registration of Tracker and Image Point-Sets

The resulting tracker and image point-sets are related by an image-to-world registration. The method of registration in this study used the rigid, point-based method described by Horn[5]. Good registration was demonstrated in a study involving 8 markers placed in non-collinear configurations which the configuration centroid was in close proximity to the surgical target.[6]

IV. EXPERIMENTAL METHODS

A. Image-to-World Registration Techniques

Two methods of point-set localization were compared: the conventional manual technique and the automatic projection-based technique. In the manual technique, localization of divot markers defined the registration of image and tracker point-sets. The image point-set was defined as the average of 10 manual localizations of all 8 divot markers in the image, known as the "true" locations of the divot markers. The tracker point-sets were defined by the manual localization of the coinciding divot markers 10 times by the tracking system using a trackable pointer. Each of the tracker point-sets was registered to the "true" point-set.

Automatic registration co-localized tracker and image point-sets. The tracker point-set (reflective markers) was localized 10 times, and each set was rigidly registered to the image point-set (BB markers).

B. Marker Configurations

Two experiments were performed to characterize the accuracy and precision of the automatic registration algorithm. The first validated the automatic technique in comparison to the manual approach. Eight MM markers were placed on the surface of the head phantom, M1-M8 in Fig 4(a), with divot markers placed immediately adjacent. Divot markers were also affixed to the surface as target points, T1–T4 in Fig. 4, for measurement of TRE in both techniques. This configuration of MM markers, referred to as "In-FOV."

The second experiment explored the possibility of placing MM markers in configurations that are potentially better suited to head and neck surgery. Three "Out-FOV" configurations were considered in which MM markers were attached to the curved plate. The rationale for this approach was: i.) to overcome the lack of rigid anatomy inferior to the cranium; ii.) to

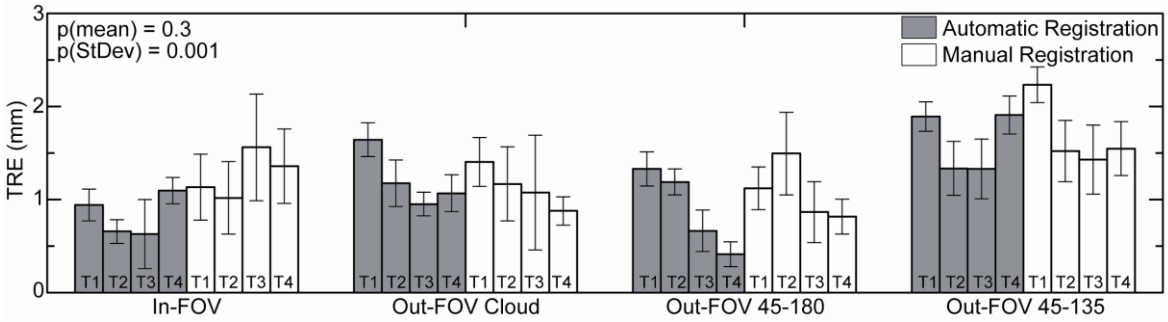

Figure 5. TRE measurements for all target points and marker configurations. The bars represent the mean and the error bars the standard deviation. The automatic and manual registration methods exhibit overall mean TRE of 1.14 and 1.29 mm with overall average standard deviation of 0.20 and 0.34 mm, respectively.

place the configuration centroid nearer to subcranial targets; and iii.) to allow flexible marker configurations that would be surgically unobtrusive. The Out-FOV MM marker configurations are referred to as "Cloud," "45-180," and "45-135," as illustrated in Fig. 4(b-d). Divot markers were placed adjacent to each MM marker for comparison to the manual localization technique. While the Out-FOV markers may not appear within the 3D FOV of the CBCT image, they do present in a subset of the CBCT projection data.

C. Target Registration Error

An important metric of accuracy of image-to-world registration is the TRE. TRE is the post-registration distance between homologous image and tracker points other than the registration point-sets. TRE measurements were performed for each target marker, T1-T4 in Fig. 4, for both the manual and automatic registration techniques and all configurations.

V. RESULTS

The TRE was measured for both registration techniques for each of the 4 marker configurations using the 4 target divot markers. As shown in Fig. 5, the TRE for the automatic technique was consistently at or below that of the conventional manual technique, with an overall mean of 1.14 ± 0.20 mm compared to 1.29 ± 0.34 mm. The superior TRE for the automatic registration technique is not statistically significant ($p = 0.3$) and suggests greater reproducibility. The results agree with TRE reported for an automatic registration technique (2.11 ± 0.13 mm) which localized markers directly in the CBCT image.[7] The reduced TRE measured in the current work is likely associated with intrinsically higher resolution of the projection data compared to 3D reconstructions, the position of the tracking system, and variations in trackable tools.

VI. DISCUSSION

The automatic registration technique exhibits comparable accuracy and improved reproducibility to that of the conventional manual technique. Although the timescales were not rigorously evaluated, the automatic technique is almost certainly less time consuming. The conventional procedure takes minutes to complete, compared to seconds for the automatic procedure. In addition, much of the process can be conducted in parallel with CBCT image reconstruction and thereby automatically update the registration with each CBCT scan. It is foreseeable that the registration process can operate seamlessly without user intervention and allow accurate surgical navigation in the context of up-to-date intraoperative images while reducing the registration workflow burden.

VII. ACKNOWLEDGEMENTS

The authors extend sincere thanks to G. Bootsma, S. Nithiananthan and Dr. H. Chan for help with the C-arm, tracking, and visualization systems. The work was supported by the Guided Therapeutics program at University Health Network, an NSERC graduate scholarship, and the National Institutes of Health and published in *Medical Physics* vol. 36, issue 5, 2009.

REFERENCES

[1] R. Sindwani, R.D. Bucholz, "The next generation of navigational technology" Otolaryngologic Clinics of North America, vol. 38, issue 3, pp. 551-562, 2005

[2] R.L. Galloway, "The process and development of image-guided procedures" Ann. Rev. of Biomed. Eng., vol. 3, pp. 83-108, 2001

[3] J.H. Siewerdsen et al, "Flat-panel cone-beam CT: A novel imaging technology for image-guided procedures," Proc. of SPIE Visualization, Display, and Image-Guided Procedures, vol. 4319, pp. 435-444, 2001

[4] M.J. Daly, J.H. Siewerdsen, Y.B. Cho, D.A. Jaffray J.C. Irish, "Geometric calibration of a mobile c-arm for intraoperative cone beam CT," Med. Phy., vol. 35, issue 5, pp. 2124-2136, 2008

[5] B. K. Horn, "Closed-form solution of absolute orientation using unit quaternions," Journal of the Optical Society of America A, vol. 4, issue 4, pp. 629-642, 1987

[6] N. M. Hamming, M.J. Daly, J.C. Irish, J.H. Siewerdsen, "Effect of Fiducial Configuration on Target Registration Error in Intraoperative Cone-Beam CT Guidance of Head and Neck Surgery," IEEE Proc. of Eng. in Med. and Bio. Soc., pp. 3643-3648, 2008

[7] G. Bootsma, J.H. Siewerdsen, M.J. Daly, D.A. Jaffray, "Initial investigation of an automatic registration algorithm for surgical navigation," IEEE Proc. of Eng. in Med. and Bio. Soc., vol. 1, pp. 3638-3642, 2008